Oceanic Rings and Jets as Statistical Equilibrium States

ANTOINE VENAILLE

CNRS, Laboratoire de Physique ENS-Lyon, Lyon, France, and GFDL, AOS, Princeton, New Jersey

FREDDY BOUCHET

CNRS, Laboratoire de Physique ENS-Lyon, Lyon, France

(Manuscript received 16 September 2010, in final form 23 March 2011)

ABSTRACT

Equilibrium statistical mechanics of two-dimensional flows provides an explanation and a prediction for the self-organization of large-scale coherent structures. This theory is applied in this paper to the description of oceanic rings and jets, in the framework of a 1.5-layer quasigeostrophic model. The theory predicts the spontaneous formation of regions where the potential vorticity is homogenized, with strong and localized jets at their interface. Mesoscale rings are shown to be close to a statistical equilibrium: the theory accounts for their shape, drift, and ubiquity in the ocean, independently of the underlying generation mechanism. At basin scale, inertial states presenting midbasin eastward jets (and then different from the classical Fofonoff solution) are described as marginally unstable states. In that case, considering a purely inertial limit is a first step toward more comprehensive out-of-equilibrium studies that would take into account other essential aspects, such as wind forcing.

1. Introduction

Large-scale coherent structures are ubiquitous in the ocean. Understanding the physical mechanism underlying their formation and persistence remains a major theoretical challenge.

At mesoscale, oceanic turbulence is mostly organized into westward-propagating rings, as for instance revealed by altimetry (Chelton et al. 2007). Because typical eddy turnover times are much shorter than dissipation and forcing time scales, these rings can be studied in the inertial limit, for which forcing and dissipation are neglected.

At basin scale, the dynamics are strongly influenced by forcing and dissipation: wind forcing plays the leading role in setting the gyre structures through the Sverdrup balance, and the concomitant effect of planetary vorticity gradients and dissipation explains their westward intensification (Pedlosky 1998). Because none of these mechanisms are conservative processes, the inertial approach does not take these essential aspects into account. Conversely, existing theories give no clear explanation of the existence of strong and robust eastward jets in the inertial part of these currents. The classical wind-driven ocean theory and the inertial approach both give an incomplete picture and complement each other. A useful step toward a comprehensive nonequilibrium theory that would combine both approaches is to study midbasin eastward jets in the inertial limit. Such is the focus of this paper.

On the one hand, the problem of the self-organization of a turbulent flow involves a huge number of degrees of freedom coupled together via complex nonlinear interactions. This situation makes any deterministic approach illusory if not impossible. On the other hand, there can be abrupt and drastic changes in the large-scale flow structure when varying a single parameter such as the energy of the flow. It is then appealing to study this problem with a statistical mechanics approach, which reduces the problem of large-scale organization of the flow to the study of states depending on a few key parameters only.

Such a theory exists: this is the Robert–Sommeria–Miller (RSM) equilibrium statistical mechanics (Robert 1990; Miller 1990; Robert 1991; Robert and Sommeria 1991). From the knowledge of the energy and the global distribution of potential vorticity levels provided by an initial condition, the theory predicts the large-scale flow as the most probable outcome of turbulent mixing. Here

Corresponding author address: Antoine Venaille, Phys ENS-Lyon, 46 Allée d'Italie, 69007 Lyon, France.
E-mail: antoine.venaille@ens-lyon.org

DOI: 10.1175/2011JPO4583.1

we ask the following question: can rings and jets be interpreted as RSM statistical equilibria in the framework of a 1.5-layer quasigeostrophic (QG) model?

The first attempt to use equilibrium statistical mechanics ideas to explain the self-organization of two-dimensional (2D) turbulence was performed by Onsager (1949) in the framework of the point vortex model. To treat flows with continuous vorticity fields, another approach has been proposed by Kraichnan in the framework of the truncated Euler equations (Kraichnan and Montgomery 1980), which has then been applied to quasigeostrophic flows over topography (Salmon et al. 1976; Carnevale and Frederiksen 1987). The truncation has a drastic consequence: only the energy and the enstrophy are conserved quantities, whereas any function of the vorticity is conserved for the Euler equation. The energy–enstrophy statistical theory predicts the emergence of large-scale mean flows above topography, characterized by a linear relationship between streamfunction and potential vorticity.

The existence of such a linear relation was assumed by Fofonoff (1954) for analytical convenience, in earlier work on inertial ocean circulation, independently of statistical mechanics approaches. Fofonoff was able to compute explicitly an inertial solution in the low energy limit. The emergence of such flows has then been observed in numerical simulations of freely evolving quasigeostrophic flows (Zou and Holloway 1994; Wang and Vallis 1994). The energy–enstrophy statistical theory has therefore been proven successful to interpret these Fofonoff flows as statistical equilibria. However, Fofonoff flows are not observed in the real ocean.

There exists actually a richer variety of energy–enstrophy states, as revealed by the computations of solutions in various configurations (see, e.g., Majda and Wang 2006; Frederiksen and O'Kane (2008), and references therein). The computation of any equilibrium state characterized by a linear q–ψ relation for a given energy and circulation (which includes the previous solutions but not only) has been performed recently for a large class of models including the 1.5-layer QG equations (Venaille and Bouchet 2011; Naso et al. 2010). None of the observed inertial features of oceanic flows, such as coherent rings and midbasin eastward jets, were found in this class of equilibrium states.

For the Euler or QG dynamics, a major drawback of energy–enstrophy statistical theories is the loss of the additional invariants of the dynamics. A first attempt to include the effect of a higher-order invariant was proposed by Carnevale and Frederiksen (1987). The generalization of Onsager's ideas to the Euler and quasigeostrophic equations with continuous vorticity field, taking into account all invariants, has led to the RSM theory (Robert 1990; Miller 1990; Robert 1991; Robert and Sommeria 1991) [see Eyink and Sreenivasan (2006), Majda and Wang (2006), and Marston (2011) for recent reviews and references].

An essential point of the RSM approach is that it makes a distinction between fine-grained potential vorticity distribution on one hand, which is conserved by inviscid flows, and coarse-grained distribution of potential vorticity on the other hand, which is not conserved. This is in complete agreement with the classical and well-documented fact that potential vorticity invariants cascade toward smaller and smaller scales (both for inviscid and dissipative flows), (see, e.g., Chavanis 2008). Actually, the equilibrium statistical mechanics predicts the ratio of potential vorticity invariants that remains to the large scale and the ratio that cascades to smaller and smaller scales for an inviscid dynamics.

Computing the RSM equilibrium states requires the resolution of a variational problem with an infinite number of constraints. This practical difficulty has been overcome by treating canonically other invariants than the energy, which lead to a variational easier to solve (Ellis et al. 2000). This approach is sometimes referred to as statistical mechanics with prior vorticity distribution (Turkington 1999; Ellis et al. 2002; Majda and Wang 2006; Chavanis 2008). Any equilibrium state with prior vorticity distribution can be interpreted as an RSM equilibrium state (Bouchet 2008). This is therefore a very useful trick to compute the equilibrium states. However, we think that a physical interpretation of the prior vorticity distribution is problematic, because it would require us to define what a bath of potential vorticity is. In the case of an isolated system (e.g., a freely evolving inviscid flow), the relevant ensemble to consider is the one taking into account all the constraints of the dynamics. For this reason, we ultimately interpret the equilibrium states in terms of the RSM theory.

Several studies (e.g., Abramov and Majda 2003; Dubinkina and Frank 2010) have specifically addressed the importance of higher potential vorticity moments for the equilibrium states. Taking into account these additional dynamical invariants provides a much richer variety of equilibrium states than previous energy–enstrophy theories. It has been proven useful to describe the stratospheric polar vortex (Prieto and Schubert 2001), the self-organization following deep convection events (Dibattista and Majda 2000), or Jupiter's Red Great Spot (Bouchet and Sommeria 2002; Turkington et al. 2001).

Most of oceanic coherent structures are surface intensified, with most of their kinetic energy located above the thermocline. In addition, eastward jets and rings are characterized by a jet width on the order of the first baroclinic Rossby radius of deformation. In this paper, we consider the simplest ocean model that takes into account this vertical structure and this typical horizontal length scale: namely an equivalent barotropic, 1.5-layer QG model.

We consider the limit of small Rossby radius of deformation, which allows analytical computations of statistical equilibria, following the work of Bouchet and Sommeria (2002). This assumption provides important insights for more general situations, even when such a scale separation does not exist. This is also a first step before considering the shallow-water model, which is consistent with the scale separation between the Rossby radius of deformation and the domain scale.

In the limit of small Rossby radius of deformation, it has been shown that the computation of RSM statistical equilibria can be simplified into a Van der Waals–Cahn–Hilliard variational problem (Bouchet 2008). These variational problems explain the formation and the shape of bubbles in thermodynamics. The existence of this formal analogy has been very fruitful in the description of Jovian vortices. This paper puts forward this approach in the oceanic context.

The paper is organized as follows: Equilibrium statistical mechanics of the 1.5-layer QG model is presented in the second section. The method to compute analytically statistical equilibrium states in the limit of small Rossby radius of deformation is presented on the third section. It allows for a justification of the potential vorticity homogenization theory of Rhines and Young (1982) without invoking any dissipation mechanism. The application to oceanic rings is discussed in a fourth section, by considering the case of a zonal channel on a beta plane. The application to midbasin eastward jets is discussed in a fifth section, by considering the case of a closed domain. Notations and symbols are referenced in Table 1.

2. Statistical mechanics of the 1.5-layer equivalent barotropic QG model

a. *The 1.5-layer QG model, its dynamical invariants, and its dynamical equilibria*

The simplest possible inertial midlatitude ocean model taking into account the stratification of the oceans and the sphericity of the earth is considered in this paper. This is the unforced, undissipated, 1.5-layer QG model on a beta plane,

$$\frac{\partial q}{\partial t} + \mathbf{v}\cdot\nabla q = 0, \quad \text{with} \quad \mathbf{v} = \mathbf{e}_z \times \nabla\psi, \quad \text{and} \quad (1)$$

$$q = \nabla^2\psi - \frac{\psi}{R^2} + \beta y. \quad (2)$$

For the boundary conditions, two cases will be distinguished, depending on the domain geometry $\mathcal{D}$. In the case of a closed domain, there is an impermeability constraint (no flow across the boundary), which amounts to a constant streamfunction along the boundary. To simplify the presentation, the condition $\psi = 0$ at boundaries will be considered.[1] In the case of a zonal channel, the streamfunction ψ is periodic in the x direction, and the impermeability constraint applies on northern and southern boundaries. In the remaining, length scales are nondimensionalized such that the domain area $|\mathcal{D}|$ is equal to one.

According to Noether's theorem, each symmetry of the system is associated with the existence of a dynamical invariant (see, e.g., Salmon 1998). These invariants are crucial quantities, because they provide strong constraints for the flow evolution. Starting from (1), (2), and the aforementioned boundary conditions, one can prove that QG flows conserve the energy,

$$E = \frac{1}{2}\int_{\mathcal{D}} d\mathbf{r}\left[(\nabla\psi)^2 + \frac{\psi^2}{R^2}\right] = -\frac{1}{2}\int_{\mathcal{D}} d\mathbf{r}(q - \beta y)\psi$$
$$\text{where} \quad d = \nabla(\partial_x, \partial_y) \quad (3)$$

Additionally, the QG dynamics (1) is a transport by an incompressible flow, so that the area $\gamma(\sigma)d\sigma$ occupied by a given vorticity level σ is a dynamical invariant. The quantity $\gamma(\sigma)$ will be referred to as the global distribution of potential vorticity. The conservation of the distribution $\gamma(\sigma)$ is equivalent to the conservation of any moment of the potential vorticity $\int_{\mathcal{D}} d\mathbf{r}\, q^n$ and is related to particle relabeling symmetry (Ripa 1981; Salmon 1998).

The stationary points of the QG Eq. (1), referred to as dynamical equilibrium states, satisfy $\mathbf{v}\cdot\nabla q = \nabla\psi \times \nabla q = 0$. It means that dynamical equilibria are flows for which streamlines are isolines of potential vorticity. Then, any state characterized by a q–ψ functional relationship is a dynamical equilibrium.

At this point, we need a theory (i) to support the idea that the freely evolving flow dynamics will effectively self-organize into a dynamical equilibrium state, (ii) to determine the q–ψ relationship associated with this dynamical equilibrium, and (iii) to select the dynamical equilibria that are likely to be observed. This is the goal and the achievement of equilibrium statistical mechanics theory, which is presented in the next subsection.

b. *The equilibrium statistical mechanics of RSM*

The RSM statistical theory is introduced on a heuristic level in the following. There exists rigorous justifications of the theory (see, e.g., Bouchet and Corvellec 2010, and references therein).

[1] The physically relevant boundary condition should be $\psi = \psi_{\text{fr}}$, where ψ_{fr} is determined by using the mass conservation constraint $\int d\mathbf{r}\,\psi = 0$ (ψ is proportional to interface variations). Taking $\psi = 0$ does not change quantitatively the solutions in the domain bulk but only the strength of boundary jets.

TABLE 1. Symbols and notations used in the text.

Symbol	Definition
$\mathbf{e}_{x,y,z}$	unit vectors in the meridional (x), zonal (y), and vertical (z) directions
$\mathbf{r} = (x, y)$	coordinate of a point, with $\mathbf{V} = (\partial_x, \partial_y)$
t	time coordinate
R	Rossby radius of deformation
f_0	Coriolis parameter
β	planetary vorticity gradient
$\mathcal{D}$	domain where the flow takes place (with $\lvert\mathcal{D}\rvert = 1$)
$\mathbf{u}(\mathbf{r})$	velocity field
$q(\mathbf{r}, t)$	(fine grained) potential vorticity field
σ	level of potential vorticity, with $\sigma \in \sum =]-\infty, +\infty[$
$\overline{q}, \overline{\psi}$	(coarse grained) mean-field potential vorticity and streamfunction
E	energy of the flow
$\gamma(\sigma)$	global distribution of potential vorticity levels
$\rho(\mathbf{r}, \sigma)$	probability distribution function
$\mathcal{S}[\rho]$	mixing entropy
$\mathcal{N}[\rho] = N$	normalization constraint
$D_\sigma[\rho] = \gamma(\sigma)$	constraint on global potential vorticity distribution
$\varepsilon[\rho] = E$	constraint on the energy
$\zeta(\mathbf{r})$	Lagrange multiplier associated with the normalization $\mathcal{N}$
$\alpha(\sigma)$	Lagrange multiplier associated with the global vorticity distribution D_σ
λ	Lagrange multiplier associated with the energy ε
$g_\alpha(\lambda\psi)$	q–ψ relation at equilibrium
$\phi = \psi/R^2$	rescaled streamfunction
$\mathcal{F}[\phi]$, F	free energy functional and equilibrium free energy
$f(\phi)$	specific free energy
$C = -\lambda R^2$	rescaled Lagrange multiplier associated with the energy constraint
$M = \int_{\mathcal{D}} d\mathbf{r}\, \phi$	constraint for ϕ
μ	Lagrange parameter associated with M
ϕ_1, ϕ_2	values of ϕ in a given phase
q_1, q_2	values of q in a given phase
A_1, A_2	domain (and area) occupied by a given phase
L	perimeter of the interface between phases
r	curvature radius of the interface
η	Lagrange multiplier associated with the constraint on A_2 when minimizing L
$\tau = R\tilde{\tau}$	coordinate across the interface
$\phi_{\text{jet}}(\tau)$	jet profile
$U_{\text{jet}} = (\phi_2 - \phi_1)R$	velocity of the jet
$\mathcal{F}_{int} = cRL(\phi_2 - \phi_1)^2$	free energy of the interface, with $c \sim 1$
$\mathcal{L}[q] = \mathcal{L}^i = \mathcal{L}^f$	constraint on the linear momentum (i is initial and f is final)
y_f, y_{jet}	latitude of the ring center of jet latitude
$\tilde{\beta} = \beta/R^2$	rescaled beta coefficient
$\mathcal{F}_\beta$	contribution of the beta term to the free energy
$l(x)$	perturbation of the zonal interface
$\mathcal{F}_R = \mathcal{F}_{\text{int}} + \mathcal{F}_\beta$	first-order corrections to the free energy
L_x, L_y	zonal and meridional extension of the closed domain
L_{ring}	diameter of the ring

A microscopic state is defined by its potential vorticity field $q(\mathbf{r})$. If taken as an initial condition, such a fine-grained field would evolve toward a state with filamentation at smaller and smaller scales while keeping in general a well-defined large-scale organization. Then, among all the possible fine-grained states, an overwhelming number are characterized by these complicated small-scale filamentary structures. This phenomenology gives a strong incentive for a mean-field approach, in which the flow is described at a coarse-grained level.

For that purpose and following Robert and Sommeria (1991), we introduce the probability $\rho(\sigma, \mathbf{r})d\sigma$ to measure a potential vorticity level σ at a point $\mathbf{r} = (x, y)$. The probability density field ρ defines a macroscopic state of the system. The corresponding averaged potential vorticity field, also referred to as coarse grained or mean field, is

$$\overline{q}(\mathbf{r}) = \int_{\Sigma} d\sigma\, \sigma\rho(\sigma, \mathbf{r}), \tag{4}$$

with the average streamfunction $\overline{\psi}$ defined by $\overline{q} = \nabla^2\overline{\psi} - \overline{\psi}/R^2 + \beta y$ and where $\sum =]-\infty, +\infty[$. Many microscopic states q can be associated with a given macroscopic state ρ. The cornerstone of the RSM statistical theory is the computation of the most probable state ρ_{eq}, which maximizes the mixing entropy given by the Boltzmann–Gibbs formula,

$$\mathcal{S}[\rho] \equiv -\int_{\mathcal{D}} d\mathbf{r} \int_{\Sigma} d\sigma\, \rho \log\rho, \tag{5}$$

while satisfying the constraints associated with each dynamical invariant. The mixing entropy (5) is a quantification of the number of microscopic states q corresponding to a given macroscopic state ρ. The state ρ_{eq} is not only the most probable one: an overwhelming number of microstates are effectively concentrated close to it (Michel and Robert 1994). This gives the physical explanation and the prediction of the large-scale organization of the flow.

In the remaining of this paper, the expression ''global entropy maximum,'' or stable equilibrium state, will be used for any global maximizer ρ of the entropy (5) satisfying the constraints. The expression ''local entropy maximum,'' or metastable equilibrium state, will be used for any state ρ that is a local maximizer of the entropy (5), satisfying the constraints.

To compute statistical equilibria, the constraints must be expressed in term of the macroscopic state ρ:

- the local normalization $N[\rho](\mathbf{r}) \equiv \int_{\Sigma} d\sigma\, \rho(\sigma, \mathbf{r}) = 1$;
- the global potential vorticity distribution $D_{\sigma}[\rho] \equiv \int_{\mathcal{D}} d\mathbf{r}\, \rho(\sigma, \mathbf{r}) = \gamma(\sigma)$; and
- the energy $\mathcal{E}[\rho] \equiv -\frac{1}{2}\int_{\mathcal{D}} d\mathbf{r} \int_{\Sigma} d\sigma\, \rho(\sigma - \beta y)\overline{\psi} = E$.

Because of the overwhelming number of states with only small-scale fluctuations around the mean-field potential vorticity and because energy is a large-scale quantity, contributions of these fluctuations to the total energy are negligible with respect to the mean-field energy (Robert and Sommeria 1991).

The first step toward computations of RSM equilibria is to find critical points ρ of the mixing entropy (5). To take into account the constraints, one needs to introduce the Lagrange multipliers $\zeta(\mathbf{r})$, $\alpha(\sigma)$, and λ associated with the local normalization, the conservation of the global vorticity distribution, and the conservation of the energy, respectively. Critical points are solutions of

$$\forall\delta \quad \rho\delta\mathcal{S} - \lambda\delta\mathcal{E} - \int_{\Sigma} d\sigma \times \alpha\delta D_{\sigma} - \int_{\mathcal{D}} d\mathbf{r}\, \zeta\delta N = 0, \tag{6}$$

where first variations are taken with respect to ρ. This leads to $\rho = N \exp[\lambda\sigma\psi(\mathbf{r}) - \alpha(\sigma)]$, where N is determined by the normalization constraint ($\int d\sigma\, \rho = 1$). Finally, using (4), one finds that statistical equilibria are dynamical equilibria characterized by a functional relation between potential vorticity and streamfunction,

$$\overline{q} = \frac{\displaystyle\int_{\Sigma} d\sigma \times \sigma e^{\lambda\sigma\psi(\mathbf{r}) - \alpha(\sigma)}}{\displaystyle\int_{\Sigma} d\sigma \times e^{\sigma\lambda\psi(\mathbf{r}) - \alpha(\sigma)}} \equiv g_{\alpha}(\lambda\overline{\psi}). \tag{7}$$

It can be shown that g_{α} is a monotonic, increasing, and bounded function of $\lambda\overline{\psi}$ for any global distribution $\gamma(\sigma)$ and energy E. These critical points can either be entropy minima, saddle, or maxima. To find statistical equilibria, one needs then to select the entropy maxima.

At this point, two different approaches could be followed. The first one would be to consider a given small-scale distribution $\gamma(\sigma)$ and energy E and then to compute the statistical equilibria corresponding to these parameters. In practice, especially in the geophysical context, one does not have empirically access to the fine-grained vorticity distribution but rather to the q–ψ relation (7) of the large-scale flow. The second approach, followed in the remaining of this paper, is to study statistical equilibria corresponding to a given class of q–ψ relations.

More precisely, we will consider the class of q–ψ relations that admit an inflexion point, referred to as ''tanh like'' relations (see Fig. 1). When the global distribution $\gamma(\sigma)$ is a double-delta function (a two-level system), one can explicitly show that the q–ψ relation is a tanh function (Bouchet and Sommeria 2002), but the actual class of initial conditions associated with tanh-like relations is expected to be much larger. A pragmatic point of view is that these tanh-like relations are the ones that allow for statistical equilibria characterized by fronts of potential vorticity. In that respect, there is the relevant class of q–ψ relations to describe either rings or zonal jets.

c. *Simplification of the variational problem*

As explained in the introduction, a widely used method to solve variational problems with many constraints (such as the RSM variational problem) is to consider a dual variational problem, which has the same critical points as the initial one but is less constrained. Any solution of the less constrained (easier to solve) problem is a solution of the more constrained problem (see, e.g., Ellis et al. 2000).

Let us, for instance, consider the ensemble of rescaled streamfunction fields $\phi = \psi/R^2$ that satisfy the constraint $\int_{\mathcal{D}} d\mathbf{r}\, \phi = M$. This constraint is equivalent to the conservation of the first moment of potential vorticity $\int_{\mathcal{D}} d\mathbf{r}\, q$, at

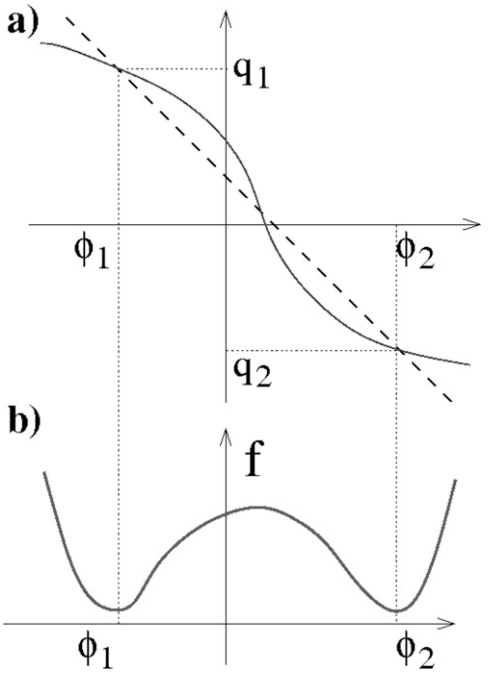

FIG. 1. (a) In this paper, we consider the class of q–ϕ relations (with $\phi = \phi/R^2$) having a tanh-like shape: namely, (i) decreasing with ϕ, (ii) bounded for $\psi \to \pm\infty$, and (iii) with a single inflection point. In addition, we assume that the slope at the inflection point is sufficiently steep, so that the q–ϕ relation represented as a solid line crosses three times the dashed line $q = -\phi - \mu$. (b) The double-well shape of the specific free energy $f(\phi)$ appearing in the expression of the free energy functional (8). This function is related to the q–ψ relation through Eq. (10). The Lagrange parameter μ is chosen such that the specific free energy of the two minima are the same $[f(\phi_1) = f(\phi_2)]$, which allows for phase coexistence.

leading order in R. Let us then look for the minimizers of the free energy functional

$$\mathcal{F} = \int_{\mathcal{D}} d\mathbf{r}\left[\frac{R^2}{2}(\nabla\phi)^2 + f(\phi) - \beta\phi y\right], \tag{8}$$

where $f(\phi)$ is a specific free energy to be defined precisely in the next paragraph. This provides a variational problem

$$F = \min_{\phi}\left\{\mathcal{F}[\phi] \Big| \int_{\mathcal{D}} d\mathbf{r}\,\phi = M\right\}, \tag{9}$$

which is much simpler than the one of the RSM statistical theory, because only one constraint is kept. Critical points of this problem are solutions of $\delta\mathcal{F} - \mu\int_{\mathcal{D}} d\mathbf{r}\,\delta\phi = 0$, for any perturbation $\delta\phi$, where α is the Lagrange multiplier associated with the constraint. A part integration and the relation $q = R^2\nabla^2\phi - \phi + \beta y$ give $\delta\mathcal{F} = \int d\mathbf{r}\,[f'(\phi) - \phi - q]\delta\phi$. Critical points therefore satisfy the relation $q = f'(\phi) - \phi - \mu$. These critical points are the same as the RSM critical points given by Eq. (7), provided that

$$f'(\phi) = g_\alpha(\lambda R^2\phi) + \phi + \mu. \tag{10}$$

This relation defines the specific free energy f. One can see that the tanh-like shape of g_α with a sufficiently steep slope at its inflection point leads to a double-well shape for f, as illustrated in Fig. 1. This double-well shape is an important ingredient for the computation of statistical equilibria in the following.

It has been proven by Bouchet (2008) that, for each minimizer ϕ of the variational problem (9), there exists a set of constraints E, $\gamma(\sigma)$ such that ϕ is the mean-field streamfunction of the RSM statistical equilibrium state ρ associated with the constraints E, $\gamma(\sigma)$. In other words, any local (global) free energy minimizer ϕ can be interpreted as a local (global) entropy maximum state of the RSM theory.

3. Potential vorticity homogenization and jets as statistical equilibria

Assuming that there is no beta effect ($\beta = 0$) and that $f(\phi)$ has a double-well shape and considering the limit $R \ll L$ (L is the domain size), Bouchet (2001, 2008) found that the variational problem (9) becomes analogous to the Van der Waals–Cahn–Hilliard model that describes phase separation and phase coexistence in thermodynamics (Modica 1987). This formal analogy provides then an interesting physical interpretation of self-organization phenomena in geostrophic turbulence.

a. Solutions of the Van der Waals–Cahn–Hilliard variational problem

At zeroth order in R, the function $f(\phi)$ plays the dominant role in the free energy functional $\mathcal{F}$ given by (8). To minimize $\mathcal{F}$, the streamfunction ϕ must therefore be equal to one of the two minima of the specific free energy $f(\phi)$ (the points ϕ_1 and ϕ_2 in Fig. 1). Each of these minima corresponds to one phase. Without the constraint $\int_{\mathcal{D}} d\mathbf{r}\,\phi = M$, one of the two uniform solutions $\phi = \phi_1$ or $\phi = \phi_2$ would minimize $\mathcal{F}$: the system would have only one phase. However, to satisfy the constraint $\int_{\mathcal{D}} d\mathbf{r}\,\phi = M$, the system has to split into subdomains: part of it with phase $\phi = \phi_1$ and part of it with phase $\phi = \phi_2$. In terms of free energy minimization, the coexistence of these two phases is possible only if $f(\phi_1) = f(\phi_2)$. Using Eq. (10), one can always choose the Lagrange parameter μ to satisfy this condition (see Fig. 1 for a graphical interpretation). In physical space, the areas occupied by each of the phases are denoted as A_1 and A_2, respectively (see Fig. 2). These values are fixed by the constraint $\int_{\mathcal{D}} d\mathbf{r}\,\phi = M$, which gives at leading order $\phi_1 A_1 + \phi_2 A_2 = M$ and by the geometrical constraint $A_1 + A_2 = 1$ (where 1 is the area of the domain).

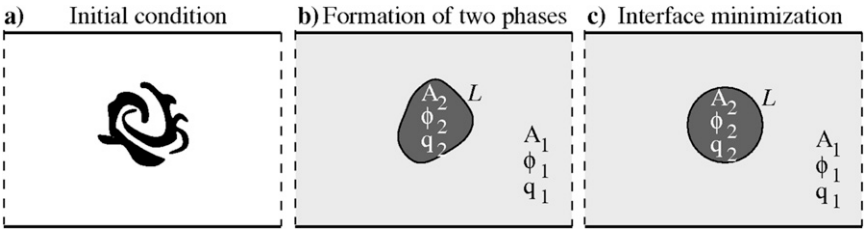

FIG. 2. Resolution of the Van der Waals variational problem (9). (a) Example of an initial condition for the potential vorticity field. Note that this initial condition could also have many levels of potential vorticity. (b) At zeroth order in R, ϕ takes two values, ϕ_1 and ϕ_2, on two subdomains, A_1 and A_2, corresponding to the coexistence of two phases of homogenized potential vorticity, q_1 and q_2. These subdomains are separated by strong jets of typical width $l_{\text{jet}} = R$ and velocity $U_{\text{jet}} = (\phi_2 - \phi_1)R$. (c) The actual shape of the structure, or equivalently the position of the jets, is obtained by minimizing its perimeter L for a fixed value of A_2.

The interface between the subdomains characterized by ϕ_1 and ϕ_2 corresponds to an abrupt variation of streamfunction. The term $R^2(\nabla\phi)^2$ in the expression (8) of the free energy $\mathcal{F}$ is negligible everywhere but around this interface, on a typical width of order R. The interface is therefore associated with a strong and localized jet directed along this interface, with a typical velocity $U_{\text{jet}} = (\phi_1 - \phi_2)R$ and a typical width R. The actual jet profile is computed in appendix A by minimizing the free energy associated with this profile. The jet gives always a positive contribution to the free energy,

$$\mathcal{F}_{\text{int}} = c(\phi_2 - \phi_1)^2 RL, \quad \text{with} \quad c \sim 1. \tag{11}$$

To minimize this interfacial free energy, the perimeter of the jet L must be minimal, taking into account the constraints given by the fixed areas A_1 and A_2. We thus look for the curve with the minimal length that bounds a given surface. The solution of this classical problem is that the interface is either a circle or a straight line.

To conclude, the computation of the statistical equilibria predicts (i) the formation of two phases of constant streamfunction, with strong and localized jets at these interface; (ii) the velocity profile across of these jets; and (iii) the shape of the interface, which is determined by an isoperimetrical problem: the minimization of the interface length for a fixed enclosed area.

b. *Link with potential vorticity homogenization theories*

The tanh-like shape of the q–ψ relations implies that subdomains of constant streamfunction are also subdomains of constant coarse-grained potential vorticity. It means that the potential vorticity is homogenized in each subdomain. Statistical mechanics provides therefore a physical explanation for the potential homogenization theory of Rhines and Young (1982), without invoking any dissipation mechanism.

In the case of freely evolving 1.5-layer QG dynamics, statistical mechanics predicts not only the spontaneous formation of regions where potential vorticity is homogenized at a coarse-grained level but also the shape of the interface between these regions, corresponding to jets, where vorticity gradients are confined. Statistical mechanics arguments also account for the irreversible nature of mixing: an overwhelming number of fine-grained microscales are associated with a given coarse-grained equilibrium state. The only effect of a weak small-scale dissipation process would be to smooth out locally fine-grained fluctuations of potential vorticity, leaving unchanged its coarse-grained structure.

Note that the formation of two subdomains of homogenized coarse-grained potential vorticity is essential to ensure the energy conservation. Importantly, any eddy parameterization based on local downgradient diffusivities could not represent this homogenization process: it would lead to the formation of a single phase of homogenized potential vorticity, which would in general not satisfy the energy constraint.

These results are complementary to previous work focusing on the dynamics of potential vorticity mixing, using chaotic advection theory (Pierrehumbert 1991). Chaotic advection theory has been proven successful to account for many observed features of potential vorticity mixing, but, unlike statistical mechanics, it provides in general no prediction for the final state of the large-scale flow, especially when there is no scale separation between mean and eddies in the initial condition.

4. Application to oceanic rings

Observations show that mesoscale oceanic rings exist everywhere in the ocean, particularly near western boundary currents, where high levels of eddy kinetic energy levels are largely associated with their presence [see, e.g., Olson (1991) for a review and Morrow et al. (2004)

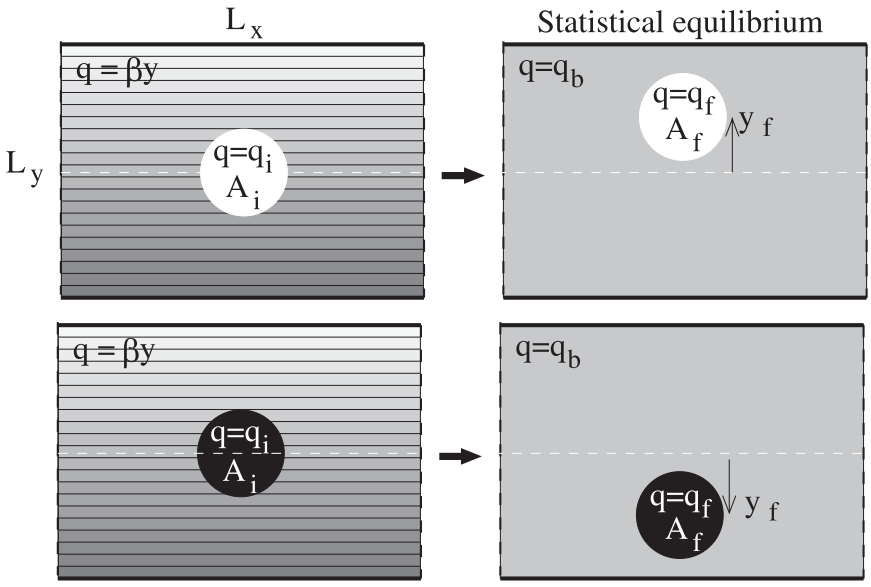

FIG. 3. Explanation of the meridional drift of rings, as a tendency to reach the statistical equilibria. (left) Initial conditions, with (top) a white disk of positive potential vorticity and (bottom) a black disk of negative potential vorticity. In both cases the disk evolves on an initial beta plane with no background flow. (right) The corresponding statistical equilibrium.

and Chelton et al. (2007) for recent altimetry measurements]. Both cyclonic and anticyclonic rings propagate westward at speed βR^2. They also present an additional small meridional drift, poleward for cyclonic rings and equatorward for anticyclonic rings.

Among others, contributions of McWilliams and Flierl (1979), Nof (1981), Flierl (1987), and Cushman-Roisin et al. (1990) have provided insights on the dynamics and on the mechanisms responsible for the generation of the rings, in a large class of models and configurations. Various dynamical mechanisms accounting for the formation of the rings have been pointed out: vortex shedding above topography, pinch-off process during the nonlinear evolution of a meandering jet, boundary layer separation, or large-scale organization of initially small turbulent disturbances. Despite these very different generation mechanisms, the striking resemblance between observed oceanic rings in very different regions of the ocean, which has long been recognized as a surprising result (Olson 1991), suggests that at least some aspect of these coherent structures can be studied independently of their generation mechanism. This is precisely the interest of statistical mechanics, which accounts for spontaneous formation of circular structures surrounded by a jet: that is, the self-organization of mesoscale turbulence into rings.

a. *The westward drift of the rings*

To show that westward-propagating circular rings can be interpreted as equilibrium states, two important ingredients must be taken into account: (i) the beta effect βy and (ii) a domain invariant by translation in the zonal direction. A drifting ring could not exist as statistical equilibria in a closed domain, because it would be destroyed when arriving on the western boundary. The zonal translational invariance of the problem has important consequences. It is shown in appendix B that a change of Galilean reference frame in the zonal direction translates as a beta effect in the expression of potential vorticity. Moreover, in a reference frame moving at velocity $-\beta R^2 \mathbf{e}_x$, the beta effect is exactly canceled out. We conclude that, in a domain invariant by translation in the zonal direction, statistical equilibria obtained by the minimization of the Van der Waals–Cahn–Hilliard variational problem (9) without beta effect are also statistical equilibria with beta effect but drifting westward at speed $V = -\beta R^2$.

b. *The poleward drift of cyclones and the equatorward drift of anticyclones*

If the flow actually reaches a local statistical equilibrium, then not only the ring is composed of a homogenized region of potential vorticity but also the background flow. In Fig. 3, the case of an isolated patch of potential vorticity ($q = q_i$ within the ring of area A_i centered on $y = 0$) on a beta plane is represented ($q = \beta y$ elsewhere). This situation is common in the ocean: for instance, when Agulhas rings arrive in quiescent regions of the Atlantic Ocean. Because the background potential vorticity is not homogenized, this state is not a statistical equilibrium state.

It is shown in the following that the observed asymmetric small meridional drift of cyclonic and anticyclonic rings can be understood as a tendency for the system to reach the statistical equilibrium [see also Schecter and Dubin (2001) for a similar argument in the context of beta-plane turbulence]. One needs for that purpose to consider the conservation of the linear momentum,

$$\mathcal{L} = \int_{\mathcal{D}} d\mathbf{r}\, qy,$$

which is the dynamical invariant associated with the zonal translational symmetry. The linear momentum of the initial condition is, at lowest order in R,

$$\mathcal{L}^i \approx \beta \int_{\mathcal{D}} d\mathbf{r}\, y^2 - \beta \int_{A_i} d\mathbf{r}\, y^2,$$

where A_i is the initial area of the ring. Considering the limit of small rings compared to the domain size, the first term of the right-hand side dominates the second one and $\mathcal{L}^i \approx \beta L_x L_y^3/24$. Assuming the statistical equilibrium is reached in the final state, the flow is made of two phases of homogenized potential vorticity: the background phase, with value $q = q_b$, and the ring's phase of area A_f, centered at latitude $y = y_f$, with value $q = q_f$ (same sign as q_i) and with $|q_f| > |q_b|$. The linear momentum of this final state is

$$\mathcal{L}^f \approx q_b \int_{\mathcal{D}} d\mathbf{r}\, y - (q_f - q_b) \int_{A_f} d\mathbf{r}\, y.$$

Finally, the linear momentum conservation $\mathcal{L}^i = \mathcal{L}^f$ gives

$$\frac{\beta}{24} L_x L_y^3 \approx -(q_f - q_b) y_f A_f.$$

Physically, this means that, for statistical mechanics reasons, the background potential vorticity has to be homogenized, which leads to a loss of linear momentum that must be compensated by a latitude shift of the ring center. Rings with negative potential vorticity [$(q_f - q_b) < 0$] decrease their latitude ($y_f < 0$), whereas rings with positive potential vorticity [$(q_f - q_b) > 0$] increase their latitude ($y_f > 0$). Then, in order to reach the statistical equilibrium, the ring has to drift northward if it is made of an initial positive potential vorticity patch and southward if it is made of an initial negative potential vorticity patch. This corresponds always to a poleward drift for cyclonic structures and an equatorward drift for anticyclonic structures, just as what is reported from altimetry measurements (Morrow et al. 2004; Chelton et al. 2007).

c. *Conclusions: Oceanic rings are local statistical equilibria*

In the ocean, the scale separation between the size of the rings and the Rossby radius of deformation is satisfied only to a limited extent. This scale separation has been assumed for technical reasons only: it allows for explicit analytical computations of the equilibria. The results obtained in this limit actually apply for far more general situations. This is confirmed by numerical computations of RSM equilibria, in which rings are obtained as local equilibria even when the scale separation is not satisfied (see, e.g., Fig. 4).

To conclude, the quasi-circular shape of oceanic rings and their westward propagation suggest that these coherent structures can be interpreted as local statistical equilibria. The existence of a meridional drift shows a departure from the prediction of the equilibrium theory. However, the fact that this drift can be interpreted as a tendency to reach to equilibrium state shows that these structures remain close to an equilibrium state. Rings are local (metastable) and not global statistical equilibria of the equivalent barotropic model (a global equilibrium would imply the coalescence of all existing rings into a single large-scale vortex) in order to minimize the total interface between the different regions of homogenized potential vorticity.

5. Application to midbasin eastward jets

Another region of the ocean where strong jets of typical width given by the Rossby radius of deformation R is localized along an interface separating two regions of homogenized potential vorticity is the inertial part of midlatitude eastward jets, such as the Kuroshio or the Gulf Stream Current. The inertial part of these currents is located in the regions where the western boundary currents separate from the coastline and self-organize downstream into a strong eastward jet. Because midbasin eastward jets fill a large part of oceanic basins and because the existence of a western boundary is an essential ingredient for their formation, one must look for statistical equilibria in a close domain in that case. In view of the applications to midbasin ocean jets, we assume a situation in which the global distribution of potential vorticity is symmetric: two phases characterized by symmetric values of streamfunction [$\phi_1 = -\phi_2 = U_{\text{jet}}/(2R)$], with each of them filling half the domain area ($A_1 = A_2 = 1/2$). We ask in this section whether configurations with midbasin eastward jets are statistical equilibria.

a. *Without beta effect, midbasin eastward jets are statistical equilibria of the QG model*

The value $\phi = \phi_{1,2}$ for the two coexisting phases is not compatible with the boundary condition $\phi = 0$. As a consequence, there exists a boundary jet in order to match a uniform phase $\phi = \phi_{1,2}$ to the boundary conditions. Just like interior jets, treated in section 3, these jets contribute to the first-order free energy, which gives the

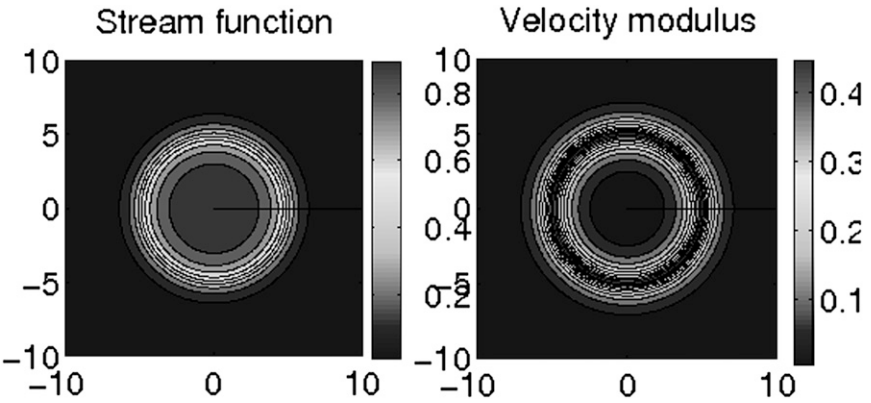

FIG. 4. Circular vortex as a statistical equilibrium of the QG model, with $R < L_{\text{ring}}$. Although analytical computations are carried in the limit $R \ll L_{\text{ring}}$, the results are expected to hold when this scale separation does not exist. It is a circular patch of (homogenized) potential vorticity in a background of homogenized potential vorticity, with two different values. (right) The velocity field has a ring structure. The width of the jet surrounding the ring has the order of magnitude of the Rossby radius of deformation R.

boundary jet structure and shape. The symmetry of the problem ($\phi_1 = \phi_2$) implies that boundary jets of each phase give the same contribution to the free energy. Because the boundary length is a fixed quantity, the free energy minimization amounts to the minimization of the interior jet length only, just as in previous subsections. The interior jet position and shape is thus given by the minimization of the interior jet length with fixed area $A_2 = ½$.

The jet has to be straight or circular. There are three possible interface configurations with straight or circular jets: (i) the zonal jet configuration (jet along the x axis), with $L = L_x$; (ii) the meridional jet configuration (jet along the y axis), with $L = L_y$; and (iii) an interior circular vortex, with $L = \sqrt{2\pi}$. The zonal jet case is a global interface minimum (and then a global equilibrium state) if and only if the aspect ratio satisfies $L_x/L_y < 1$. For $L_x/L_y > 1$, these solutions become metastable states (local entropy maximum).

We conclude that, without beta effect, midlatitude eastward jets are statistical equilibria. Because of the symmetry $\phi_1 = -\phi_2$, solutions presenting eastward and westward jets are equivalent: westward jets are also statistical equilibria.

b. *With beta effect, eastward jets become metastable or unstable*

Contrary to the case of the zonal channel, the beta effect cannot be cancelled out by a change of Galilean reference frame in the case of a closed domain. One can therefore not avoid taking into account this term in the computation of the equilibrium free energy. One can readily see on the expression (8) of the free energy that, when $\beta \neq 0$, the additional term $\mathcal{F}_\beta \equiv -\beta \int_{\mathcal{D}} d\mathbf{r}\, \phi y$ breaks the symmetry $\pm q$. The westward jet case (with $\phi < 0$ on the southern part of the domain and $\phi > 0$ on the northern part) is more favorable in terms of free energy minimization than the eastward jet case (with $\phi > 0$ in the southern part of the domain and $\phi < 0$ in the northern part): westward jets become the only global equilibria for $\beta > 0$ and aspect ratio $L_x/L_y > 1$.

Let us be more precise by considering the limit of small beta effect, with the scaling $\beta \sim R\tilde{\beta}$. With that scaling, the equivalent topography does not play any role at zeroth order in the variational problem (9). We thus still conclude that phase separation occurs, with subdomains of fixed areas A_1 and A_2, separated by jets whose transverse structure is described in appendix A. It is shown in this same appendix that the interface gives a contribution $\mathcal{F}_{\text{int}} = cRL(\phi_2 - \phi_1)^2$. Using the zeroth-order result $\phi = \phi_1$ on subdomain A_1 and $\phi = \phi_2$ on subdomain A_2, one obtains also $\mathcal{F}_\beta = -(\phi_2 - \phi_1)\beta \int_{A_2} d\mathbf{r}\, y$, plus an unimportant constant. Finally, the total first-order contribution to the free energy is

$$\mathcal{F}_R = cR(\phi_2 - \phi_1)^2 L - (\phi_2 - \phi_1)\beta \int_{A_2} d\mathbf{r}\, y. \tag{12}$$

Recalling that first variations of the length are proportional to the inverse of the curvature radius r of the interface (Gelfand and Fomin 1967), the minimization of (12), with fixed area A_2 gives

$$(\phi_2 - \phi_1)R\tilde{\beta}y + \eta = \frac{cR(\phi_2 - \phi_1)^2}{r}. \tag{13}$$

Here, η is a Lagrange parameter associated with the conservation of the area A_2.

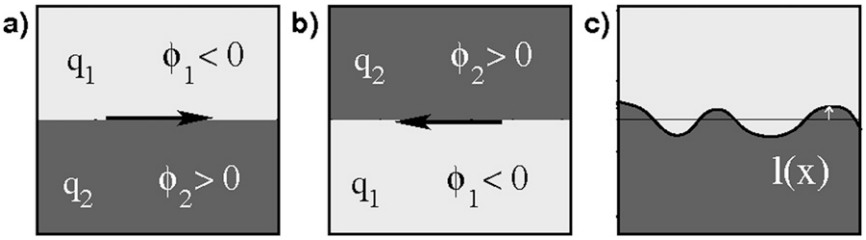

FIG. 5. (a) Eastward jet configuration; (b) westward jet configuration; and (c) perturbation of the interface for the eastward jet configuration, to determine when this solution is a local equilibrium. Without beta effect, both the eastward and the westward configurations are entropy maxima. With positive beta effect, the westward jet becomes the global entropy maximum, and the eastward jet becomes metastable provided that beta is small enough.

We conclude that zonal jets (i.e., an interface at latitude $y = y_{\text{jet}}$, with infinite curvature radius r) are solutions to this equation for $\eta = -R(\phi_2 - \phi_1)\tilde{\beta}y_{\text{jet}}$. This shows that eastward and westward jets described in the previous section are therefore still critical points of entropy maximization.

The eastward jet configuration is the one with the region A_2 below the line $y = 0$ at the center of the domain. To determine if this configuration is a local statistical equilibria, let us consider perturbations of this interface [given by the line $y = l(x)$], while keeping constant the area occupied by both phases (see Fig. 5). There are two contributions competing with each other in the expression (12) of the free energy $\mathcal{F}_R$. Any perturbation increases the jet length $L = \int dx\sqrt{1 + (l')^2}$, where $l' = dl/dx$, and then increases the first term of the free energy (12) by $\delta\mathcal{F}_{\text{int}} = cR(\phi_2 - \phi_1)^2 \int dx(l')^2$. Any perturbation decreases the second term of the free energy (12) by $\delta\mathcal{F}_\beta = -R(\phi_2 - \phi_1)\tilde{\beta} \int dx\, l^2$. If the eastward jet solution is not a free energy minimum, it exists a perturbation of the interface leading to negative variations of the free energy $\delta\mathcal{F}_R = \delta\mathcal{F}_{\text{int}} + \delta\mathcal{F}_\beta$. Let us consider the particular case $l = l_k \sin(k\pi x/L_x)$, where $k \geq 1$ is an integer. Using $U_{\text{jet}} = (\phi_2 - \phi_1)R$ and $\beta = R\tilde{\beta}$, the condition $\delta\mathcal{F}_R < 0$ gives $\beta > cU_{\text{jet}}(k\pi/L_x)^2$. The most unfavorable case is for the smallest value of k^2: that is, $k^2 = 1$.

It leads to the necessary condition $\beta > cU_{\text{jet}}\pi^2/L_x^2$ for the eastward jet solution to be unstable (in term of statistical mechanics). It can actually be shown, using less straightforward considerations, that it is also a sufficient condition for instability. The destabilizing effect of increasing values of β contrasts with its stabilizing effect in classical criteria for barotropic instability (see, e.g., Vallis 2006). It has actually been shown that such eastward jet solutions can simultaneously be unstable for statistical mechanics and stable for nonlinear perturbations (Venaille 2008).

For a fixed value of β, eastward jets are local free energy maxima if the domain zonal extension is smaller than a critical value, $L_x < \pi(cU_{\text{jet}}/\beta)^{1/2}$. The streamfunction of such a state is presented in Fig. 6. For jets like the Gulf Stream, $U_{\text{jet}} \approx 1$ m s^{-1} and $\beta \approx 10^{-11}$ m^{-1} s^{-1}. Using $c \sim 1$, the critical domain length scale upon which eastward jet become unstable is $L_x \approx 300$ km. This length is smaller than the typical zonal extension of the inertial part of the Kuroshio or Gulf Stream Current, but not by an order of magnitude, which suggests that these structures are marginally unstable. The instability is consistent with the fact that strong meanders and pinch-off process occur downstream of oceanic eastward jets. However, the marginal nature of this instability is also consistent with the overall robustness of the global structure of the flow, which becomes a statistical equilibrium when the extension of the jet is small enough.

6. Conclusions and prospects

The aim of this paper was to present a point of view complementary to existing approaches that deal with coherent structures in the ocean. It was shown that the RSM statistical mechanics provides a unified framework that may be useful to study mesoscale and basin-scale inertial flows.

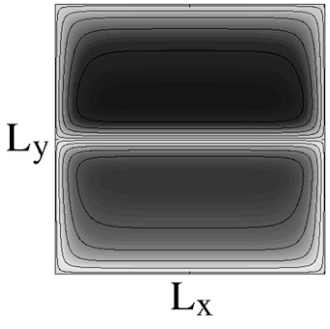

FIG. 6. Streamfunction of the solution presenting an eastward jet with beta effect, associated with Fig. 5a. The jet width is of order R. This solution is a statistical equilibrium for $L_x < \pi(U_{\text{jet}}/\beta)^{1/2}$.

The theory gives a physical explanation and a prediction for the self-organization of large-scale oceanic coherent structure, independently of the underlying generation mechanism. It predicts the formation of subdomains of homogenized potential vorticity, with intense jets at the interface. Mesoscale rings can be interpreted as local equilibrium states of the RSM theory. Their shape and their drift can be understood in this framework. Midbasin eastward jets are found marginally unstable states of the RSM theory, consistent with observations of these jets.

The interest of this approach relies on its generality (it does not depends on a particular flow configuration) and on its ability to describe qualitatively different observed regimes of self-organization, such as rings and zonal jets. The present study was achieved in the framework of a 1.5-layer QG model, which is too simplistic to describe oceanic eddies quantitatively; however, generalizations and further investigations in the framework of more complex models can be built upon these results.

A caveat of this approach is that forcing and dissipation are not taken into account in the framework of the equilibrium theory: the input of the RSM theory is given by the dynamical invariants. In the case of mesoscale rings, even if the dynamics can be considered close to an equilibrium state, forcing and dissipation play an important role in setting these dynamical invariants. In the case of basin-scale jets, their marginal instability suggests that one cannot avoid taking into account forcing and dissipation mechanisms to explain these structures. So far, the inertial part of wind-driven circulation has been mostly studied from the point of view of bifurcation theory, starting from a highly dissipated ocean and decreasing progressively frictional parameters (see, e.g., Dijkstra and Ghil 2005). We argue that this problem can be tackled with another point of view, starting from the purely inertial limit (this paper) and adding small forcing and dissipation (future work built upon Bouchet and Simonnet 2009). These two approaches are complementary and may be combined in the future in a more comprehensive nonequilibrium theory.

Acknowledgments. It is a pleasure to thank Joel Sommeria for collaboration on statistical mechanics approach, as well as Stephen Griffies, Isaac Held, and Geoffrey Vallis for interesting discussions that helped to improve the manuscript. The authors also warmly thank Nicolas Sauvage for his preliminary work during a traineeship with FB in 2005. This work was supported by the ANR program STATFLOW (ANR-06-JCJC-0037-01) and the ANR program STATOCEAN (ANR-09-SYSC-014). AV was also supported by DOE Grant DE-SC0005189 and NOAA Grant NA08OAR4320752 during part of this work.

APPENDIX A

Computation of the Jet Profile

At leading order, minimization of the free energy leads to the formation of subdomains of constant streamfunction $\phi = \phi_1$ and $\phi = \phi_2$. The interface between these subdomains is associated with strong and localized jets. Let us assume that the curvature radius of the interface is much larger than R, which allows us to neglect what happens along the interface at leading order. Calling $\tau = R\tilde{\tau}$ the coordinate in a direction along the normal to the interface, the jet profile $\phi_{\rm jet}(\tau)$ across the interface must be such that it minimizes its contribution to the total free energy (8). The jet profile is therefore determined by solving a one-dimensional variational problem,

$$\mathcal{F}_{\rm int} = LR \min_{\phi_{\rm jet}} \left\{ \int_{-\infty}^{+\infty} d\tilde{\tau} \left[\frac{1}{2} \left(\frac{d\phi_{\rm jet}}{d\tilde{\tau}} \right)^2 + f(\phi_{\rm jet}) \right] \right\}, \quad \text{(A1)}$$

where L is the perimeter of the jet and $\mathcal{F}_{\rm int}$ is the free energy associated with the existence of this interfacial jet. Critical points of this variational problem are states that cancel the first variations of the free energy with respect to $\phi_{\rm int}$. They are solutions of

$$\frac{d^2\phi_{\rm jet}}{d\tilde{\tau}^2} = \frac{df}{d\phi_{\rm jet}}. \quad \text{(A2)}$$

Making an analogy with mechanics, if $\phi_{\rm jet}$ would be a particle position and τ would be the time, then Eq. (15) would describe the conservative motion of the particle in a potential $-f$. To connect the two different phases in the bulk, on each side of the interface, one has to consider solutions with boundary conditions $\phi \to \phi_1$ for $\tau \to -\infty$ and $\phi \to \phi_2$ for $\tau \to +\infty$. There is a unique trajectory with such limit conditions. In the particle analogy, it is the trajectory connecting the two unstable fixed points ϕ_1 and ϕ_2, corresponding to the two bumps of the potential $-f$ (see Fig. 1).

The energy $(d\phi_{\rm jet}/d\tau)^2/2 - f(\phi_{\rm jet})$ is conserved during the evolution of ϕ with time τ. Using this conservation property and the boundary condition $\phi \to \phi_2$ for $\tau \to +\infty$, one obtains $f(\phi_{\rm jet}) = (d\phi_{\rm jet}/d\tau)^2/2$, plus an unimportant constant. Injecting this expression into the variational problem (14), one obtains

$$\mathcal{F}_{\rm int} = LR \int_{-\infty}^{+\infty} (d\phi_{\rm jet}/d\tau)^2 \, d\tau = cRL(\phi_2 - \phi_1)^2,$$

with $c \sim 1$. An important physical consequence is that the jet at the interface always gives a positive contribution to

the free energy of the equilibrium state, which is of order R and proportional to the interface length L.

APPENDIX B

Galilean Invariance and Beta Effect

In the case of a zonal channel, the QG Eq. (1) is invariant over a Galilean transformation in the zonal direction,

$$x \to x' = x - Vt, \quad y \to y' = y, \quad t \to t' = t.$$

The velocity is transformed as $\mathbf{v} \to \mathbf{v}' = \mathbf{v} - V\mathbf{e}_x$, which, using the relation $\mathbf{v} = \mathbf{e}_z \times \nabla\psi$, gives the transformation law for the streamfunction $\psi \to \psi' = \psi - Vy$. From the expression $q = \Delta\psi - \psi/R_2 + \beta y$, one obtains finally the transformation law for the potential vorticity $q \to q' = q + Vy/R^2$. Thus, the expression for the dynamics in the new reference frame is

$$\frac{\partial q'}{\partial t'} + \mathbf{v}' \cdot \nabla' q' = 0, \quad \text{with} \quad \mathbf{v}' = \mathbf{e}_z \times \nabla'\psi', \quad \text{and}$$

$$q' = \nabla'^2\psi' - \frac{\psi'}{R_2} + \left(\beta + \frac{V}{R^2}\right) y'.$$

REFERENCES

Abramov, R. V., and A. J. Majda, 2003: Statistically relevant conserved quantities for truncated quasigeostrophic flow. *Proc. Natl. Acad. Sci. USA,* **100,** 3841–3846.

Bouchet, F., 2001: Mécanique statistique des écoulements géophysiques. Ph.D. thesis, Université Joseph Fourier-Grenoble, 200 pp.

——, 2008: Simpler variational problems for statistical equilibria of the 2D Euler equation and other systems with long range interactions. *Physica D,* **237,** 1976–1981.

——, and J. Sommeria, 2002: Emergence of intense jets and Jupiter's Great Red Spot as maximum-entropy structures. *J. Fluid Mech.,* **464,** 165–207.

——, and E. Simonnet, 2009: Random changes of flow topology in two-dimensional and geophysical turbulence. *Phys. Rev. Lett.,* **102,** doi:10.1103/PhysRevLett.102.094504.

——, and M. Corvellec, 2010: Invariant measures of the 2D Euler and Vlasov equations. *J. Stat. Mech.,* **2010,** P08021 doi:10.1088/1742-5468/2010/08/P08021.

Carnevale, G. F., and J. S. Frederiksen, 1987: Nonlinear stability and statistical mechanics of flow over topography. *J. Fluid Mech.,* **175,** 157–181.

Chavanis, P., 2008: Statistical mechanics of 2D turbulence with a prior vorticity distribution. *Physica D,* **237,** 1998–2002.

Chelton, D. B., M. G. Schlax, R. M. Samelson, and R. A. de Szoeke, 2007: Global observations of large oceanic eddies. *Geophys. Res. Lett.,* **34,** L15606, doi:10.1029/2007GL030812.

Cushman-Roisin, B., B. Tang, and E. P. Chassignet, 1990: Westward motion of mesoscale eddies. *J. Phys. Oceanogr.,* **20,** 758–768.

Dibattista, M. T., and A. J. Majda, 2000: An equilibrium statistical theory for large-scale features of open-ocean convection. *J. Phys. Oceanogr.,* **30,** 1325–1353.

Dijkstra, H. A., and M. Ghil, 2005: Low-frequency variability of the large-scale ocean circulation: A dynamical systems approach. *Rev. Geophys.,* **43,** RG3002, doi:10.1029/2002RG000122.

Dubinkina, S., and J. Frank, 2010: Statistical relevance of vorticity conservation in the Hamiltonian particle-mesh method. *J. Comput. Phys.,* **229,** 2634–2648.

Ellis, R. S., K. Haven, and B. Turkington, 2000: Large deviation principles and complete equivalence and nonequivalence results for pure and mixed ensembles. *J. Stat. Phys.,* **101,** 999–1064.

——, ——, and ——, 2002: Nonequivalent statistical equilibrium ensembles and refined stability theorems for most probable flows. *Nonlinearity,* **15,** 239–255.

Eyink, G. L., and K. R. Sreenivasan, 2006: Onsager and the theory of hydrodynamic turbulence. *Rev. Mod. Phys.,* **78,** 87–135.

Flierl, G. R., 1987: Isolated eddy models in geophysics. *Annu. Rev. Fluid Mech.,* **19,** 493–530.

Fofonoff, N. P., 1954: Steady flow in a frictionless homogeneous ocean. *J. Mar. Res.,* **13,** 254–262.

Frederiksen, J. S., and T. J. O'Kane, 2008: Entropy, closures and subgrid modeling. *Entropy,* **10,** 635–683.

Gelfand, I., and S. Fomin, 1967: *Calculus of Variations*. Prentice Hall, 240 pp.

Kraichnan, R. H., and D. Montgomery, 1980: Two-dimensional turbulence. *Rep. Prog. Phys.,* **43,** 547–619.

Majda, A. J., and X. Wang, 2006: *Nonlinear Dynamics and Statistical Theories for Basic Geophysical Flows*. Cambridge University Press, 551 pp.

Marston, B., 2011: Looking for new problems to solve? Consider the climate. *Physics,* **4,** 20, doi:10.1103/Physics.4.20.

McWilliams, J. C., and G. R. Flierl, 1979: On the evolution of isolated, nonlinear vortices. *J. Phys. Oceanogr.,* **9,** 1155–1182.

Michel, J., and R. Robert, 1994: Large deviations for young measures and statistical mechanics of infinite dimensional dynamical systems with conservation law. *Commun. Math. Phys.,* **159,** 195–215.

Miller, J., 1990: Statistical mechanics of Euler equations in two dimensions. *Phys. Rev. Lett.,* **65,** 2137–2140, doi:10.1103/PhysRevLett.65.2137.

Modica, L., 1987: The gradient theory of phase transitions and the minimal interface criterion. *Arch. Ration. Mech. Anal.,* **98,** 123–142.

Morrow, R., F. Birol, D. Griffin, and J. Sudre, 2004: Divergent pathways of cyclonic and anti-cyclonic ocean eddies. *Geophys. Res. Lett.,* **31,** L24311, doi:10.1029/2004GL020974.

Naso, A., P.-H. Chavanis, and B. Dubrulle, 2010: Statistical mechanics of Fofonoff flows in an oceanic basin. *Eur. Phys. J.,* **80B,** 493–517.

Nof, D., 1981: On the β-induced movement of isolated baroclinic eddies. *J. Phys. Oceanogr.,* **11,** 1662–1672.

Olson, D. B., 1991: Rings in the ocean. *Annu. Rev. Earth Planet. Sci.,* **19,** 283.

Onsager, L., 1949: Statistical hydrodynamics. *Nuovo Cimento,* **6** (Suppl.), 249–286.

Pedlosky, J., 1998: *Ocean Circulation Theory*. Springer-Verlag, 459 pp.

Pierrehumbert, R. T., 1991: Chaotic mixing of tracer and vorticity by modulated travelling Rossby waves. *Geophys. Astrophys. Fluid Dyn.,* **58,** 285–319.

Prieto, R., and W. H. Schubert, 2001: Analytical predictions for zonally symmetric equilibrium states of the stratospheric polar vortex. *J. Atmos. Sci.,* **58,** 2709–2728.

Rhines, P. B., and W. R. Young, 1982: Homogenization of potential vorticity in planetary gyres. *J. Fluid Mech.,* **122,** 347–367.

Ripa, P., 1981: Symmetries and conservation laws for internal gravity waves. *American Institute of Physics Conference Proceedings,* Vol. 76, American Institute of Physics, 281–306.

Robert, R., 1990: Etats d'equilibre statistique pour l'ecoulement bidimensionnel d'un fluide parfait. *C. R. Acad. Sci.,* **1,** 575–578.

——, 1991: A maximum-entropy principle for two-dimensional perfect fluid dynamics. *J. Stat. Phys.,* **65,** 531–553.

——, and J. Sommeria, 1991: Statistical equilibrium states for two-dimensional flows. *J. Fluid Mech.,* **229,** 291–310.

Salmon, R., 1998: *Lectures on Geophysical Fluid Dynamics*. Oxford University Press, 378 pp.

——, G. Holloway, and M. C. Hendershott, 1976: The equilibrium statistical mechanics of simple quasi-geostrophic models. *J. Fluid Mech.,* **75,** 691–703.

Schecter, D. A., and D. H. E. Dubin, 2001: Theory and simulations of two-dimensional vortex motion driven by a background vorticity gradient. *Phys. Fluids,* **13,** 1704–1723.

Turkington, B., 1999: Statistical equilibrium measures and coherent states in two-dimensional turbulence. *Commun. Pure Appl. Math.,* **52,** 781–809.

——, A. Majda, K. Haven, and M. Dibattista, 2001: Statistical equilibrium predictions of jets and spots on Jupiter. *Proc. Natl. Acad. Sci. USA,* **98,** 12 346–12 350.

Vallis, G. K., 2006: *Atmospheric and Oceanic Fluid Dynamics*. Cambridge University Press, 745 pp.

Venaille, A., 2008: Mélange et circulation océanique: Une approche par la physique statistique. Ph.D. thesis, Université Joseph Fourier-Grenoble, 252 pp.

——, and F. Bouchet, 2009: Statistical ensemble inequivalence and bicritical points for two-dimensional flows and geophysical flows. *Phys. Rev. Lett.,* **102,** 104501, doi:10.1103/PhysRevLett.102.104501.

——, and ——, 2011: Solvable phase diagrams and ensemble inequivalence for two-dimensional and geophysical flows. *J. Stat. Phys.,* **143,** 346–380.

Wang, J., and G. K. Vallis, 1994: Emergence of Fofonoff states in inviscid and viscous ocean circulation models. *J. Mar. Res.,* **52,** 83–127.

Zou, J., and G. Holloway, 1994: Entropy maximization tendency in topographic turbulence. *J. Fluid Mech.,* **263,** 361–374.